

# High-Quality Animatable Dynamic Garment Reconstruction from Monocular Videos

Xiongzhen Li, Jinsong Zhang, Yu-Kun Lai, *Member, IEEE*, Jingyu Yang, *Senior Member, IEEE*, and Kun Li\*, *Member, IEEE*

**Abstract**—Much progress has been made in reconstructing garments from an image or a video. However, none of existing works meet the expectations of digitizing high-quality animatable dynamic garments that can be adjusted to various unseen poses. In this paper, we propose the first method to recover high-quality animatable dynamic garments from monocular videos without depending on scanned data. To generate reasonable deformations for various unseen poses, we propose a learnable garment deformation network that formulates the garment reconstruction task as a pose-driven deformation problem. To alleviate the ambiguity estimating 3D garments from monocular videos, we design a multi-hypothesis deformation module that learns spatial representations of multiple plausible deformations. Experimental results on several public datasets demonstrate that our method can reconstruct high-quality dynamic garments with coherent surface details, which can be easily animated under unseen poses. The code is available for research purposes at <http://cic.tju.edu.cn/faculty/likun/projects/DGarment>.

**Index Terms**—High-quality, animatable, dynamic, monocular.

## I. INTRODUCTION

3D human digitization [1]–[3] is an active area in computer vision and graphics, which has a variety of applications in the fields of VR/AR [4], [5], fashion design [6] and virtual try-on [7], [8]. A fundamental challenge in digitizing humans is the modeling of high-quality animatable dynamic garments with realistic surface details, which can be adjusted to various poses. However, traditional methods require manual processes that are time-consuming even for an expert. Therefore, it is necessary to develop new methods that efficiently generate visually high-quality animatable dynamic 3D clothing without specialized knowledge.

Learning-based clothing reconstruction methods have been demonstrated to be feasible solutions to this problem. Early methods [9]–[16] adopt a 3D scanner or a multi-view studio, but the high cost and large-scale setups prevent the widespread applications of such systems. For users, it is more convenient and cheaper to adopt a widely available RGB camera. Therefore, some works [17]–[21] attempt to reconstruct high-quality clothed humans from an RGB image or a monocular video.

However, these methods use a single surface to represent both clothing and body, which fails to support applications such as virtual try-on. Layered representation with garment reconstruction [22]–[26] is more flexible and controllable, but related research works are relatively rare. Some methods [22], [23] adopt explicit parametric models trained on the Digital Wardrobes dataset [22], which can be adjusted to various unseen poses, but they fail to reconstruct garments with high-frequency surface details (*e.g.*, wrinkles). Other methods [24], [26] try to register explicit garment templates to implicit fields to improve reconstruction quality. However, this design leaves out the body pose, which makes it impossible to control or animate the garments flexibly. In addition, all the above methods not only rely on expensive data for training, but are also bounded by domain gaps and cannot generalize well to the inputs outside the domain of the training dataset. Most importantly, none of these works meet the expectations of digitizing high-quality animatable dynamic garments that can be adjusted to various unseen poses.

Therefore, our goal is to reconstruct high-quality animatable dynamic garments from monocular videos. There are major challenges that need to be overcome to achieve this: 1) a large amount of scanned data is needed for supervision, which tends to result in domain gaps and limited performance for unseen data; 2) the absence of strong and efficient human priors increases the difficulty of estimating dynamic and reasonably wrinkled clothing directly from monocular videos; 3) recovering dynamic 3D clothes from monocular videos is a highly uncertain and inherently ill-posed problem due to the depth ambiguity.

In this paper, we propose a novel weakly supervised framework to reconstruct high-quality animatable dynamic garments from monocular videos, aiming to eliminate the need to simulate or scan hundreds or even thousands of human sequences. By applying weakly supervised training, we greatly reduce the required time of both data preparation and model deployment. To the best of our knowledge, our method is the first work to reconstruct high-quality animatable dynamic garments from a single RGB camera without depending on scanned data.

To handle dynamic garment deformation from monocular videos, we propose a learnable garment deformation network that formulates the garment reconstruction task as a pose-driven deformation problem. In particular, we utilize human body priors [27] to guide the deformation of the spatial points of garments, which makes the garment deformation more controllable and enables our model to generate reasonable deformations for various unseen poses. To alleviate the ambiguity

This work was supported in part by the National Natural Science Foundation of China (62171317 and 62122058).

\* Corresponding author: Kun Li (Email: lik@tju.edu.cn).

Xiongzhen Li, Jinsong Zhang, and Kun Li are with the College of Intelligence and Computing, Tianjin University, Tianjin 300350, China.

Yu-Kun Lai is with the School of Computer Science and Informatics, Cardiff University, Cardiff CF24 4AG, United Kingdom.

Jingyu Yang is with the School of Electrical and Information Engineering, Tianjin University, Tianjin 300072, China.

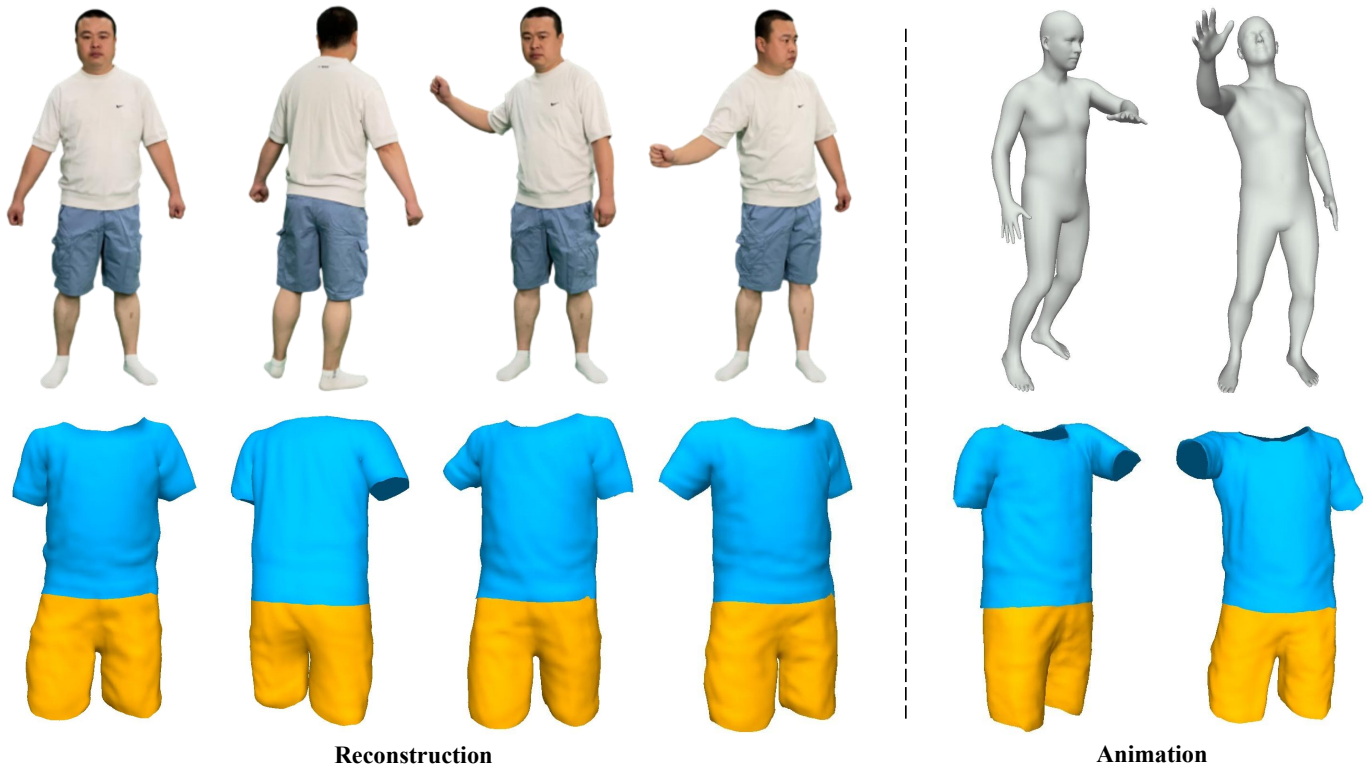


Fig. 1. Given a video of a person, our method can reconstruct high-quality and animatable garments, which enables new deformations for various unseen poses to be generated.

resulted from estimating 3D garments from monocular videos, we design a simple but effective multi-hypothesis displacement module that learns spatial representations of multiple plausible deformation. We observe that it is more reasonable to conduct multi-hypothesis estimation to obtain garment deformation than direct regression, especially for monocular camera settings, as this way can enrich the diversity of features and produce a better integration for the final 3D garments. The prior works [22], [23], [25] focus on the geometry of the clothes and do not attempt to recover the garment textures, which limits their application scenarios. Therefore, we design a neural texture network to generate high-fidelity textures consistent with the image. Experimental results on several public datasets demonstrate that our method can reconstruct high-quality dynamic garments with coherent surface details, which can be easily animated under unseen poses. An example is given in Fig. 1. *The code is available for research purposes at <http://cic.tju.edu.cn/faculty/likun/projects/DGarment>.*

Our main contributions can be summarized as follows:

- We design a weakly supervised framework to recover high-quality dynamic animatable garments from a monocular video without depending on scanned data. To the best of our knowledge, no other work meets the expectations of digitizing high-quality garments that can be adjusted to various unseen poses.
- We propose a learnable garment deformation network that formulates the garment reconstruction task as a pose-driven deformation problem based on human body priors. This enables our model to generate reasonable

deformations for various unseen poses.

- We propose a simple but effective multi-hypothesis displacement module that learns spatial representations of multiple plausible deformations. In this way, we can alleviate the ambiguity brought by estimating 3D garments based on monocular videos.

## II. RELATED WORK

### A. Clothed Human Reconstruction

Clothed human reconstruction is inevitably challenging due to complex geometric deformations under various body shapes and poses. Some methods [18], [28]–[33] explicitly model 3D humans based on parametric models like SMPL [27], and as a result may fail to accurately recover 3D geometry. Zhu *et al.* [34] combine a parametric model with flexible free-form deformation by leveraging a hierarchical mesh deformation framework on top of the SMPL model [27] to refine the 3D geometry. These methods predict more robust results, but fail to reconstruct garments with high-frequency surface details. Contrary to parametric-model-based methods, non-parametric approaches directly predict the 3D representation from an RGB image or a monocular video. Zheng *et al.* [35] propose an image-guided volume-to-volume translation framework fused with image features to reproduce accurate surface geometry. However, this representation requires intensive memory and has low resolution. To avoid high memory requirements, implicit function [19], [36] representations are proposed for clothed human reconstruction. Saito *et al.* [19] propose a pixel-aligned implicit function representation called PIFu for high-

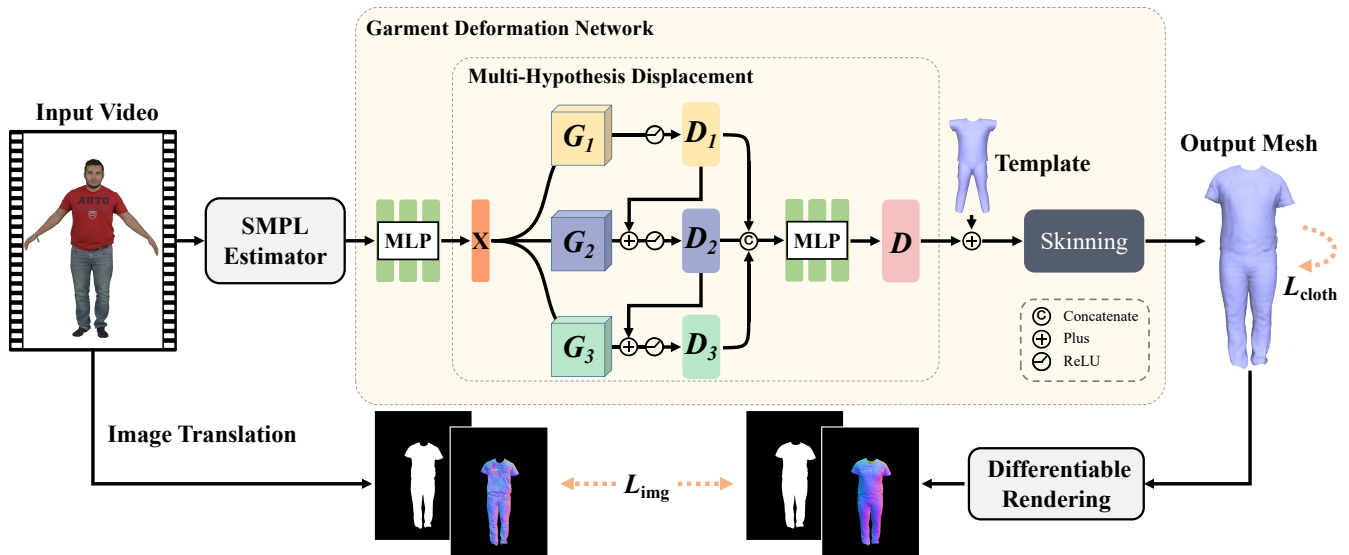


Fig. 2. Overview of our method. At the core of our method lies a learnable garment deformation network that predicts reasonable deformations for the input video. For each frame, we first design an MLP to obtain a high-level embedding  $X$  based on the SMPL pose and define three learnable matrices  $G_1, G_2, G_3$  to get three deformations  $D_1, D_2, D_3$ . Then, we connect them as the input of an MLP that outputs the final deformation  $D$ . This design can enrich the diversity of features and help produce aggregated displacements for more reasonable garment deformation. These displacements are added to the garment template, which is then skinned along the body according to pose parameters  $\theta$  and blend weights  $\mathcal{W}_c$  to produce the final result. We train the network using  $L_{img}$  and  $L_{cloth}$  loss function in a weakly supervised manner, which removes the need for ground-truth data.

quality mesh reconstructions with fine geometry details (e.g., clothing wrinkles) from images. However, PIFu [19] and its variants [37]–[43] may generate implausible results such as broken legs. Feng *et al.* [20] propose a new 3D representation, FOF (Fourier Occupancy Field), for monocular real-time human reconstruction. Nonetheless, FOF cannot represent very thin geometry restricted by the use of low-frequency terms of Fourier series. Recently, inspired by the success of neural rendering methods in scene reconstruction [44], [45], various methods [46]–[51] recover 3D clothed humans directly from multi-view or monocular RGB videos. Although these approaches demonstrate impressive performance, they fail to support applications such as virtual try-on, because they use a single surface to represent both clothing and body.

### B. Garment Reconstruction

In comparison to clothed human reconstruction using a single surface representation for both body and clothing, treating clothing as separate layers on top of the human body [22]–[26], [52]–[56] allows controlling or animating the garments flexibly and can be exploited in a range of applications. Some methods [22]–[26], [52], [53] address the challenging problem of garment reconstruction from a single-view image. Bhatnagar *et al.* [22] propose the first method to predict clothing layered on top of the SMPL [27] model from a few frames of a video trained on the Digital Wardrobes dataset. Jiang *et al.* [23] split clothing vertices off the body mesh and train a specific network to estimate the garment skinning weights, which enables the joint reconstruction of body and loose garment. SMPLicit [25] is another approach that builds a generative model which embeds 3D clothes as latent codes to represent clothing styles and shapes. As a further attempt,

Moon *et al.* [52] propose Clothwild based on SMPLicit [25] to produce robust results from in-the-wild images. Although these methods regard clothing and human body as independent layers, they fail to recover high-frequency garment geometry.

Unlike previous works, to reconstruct high-quality garment geometry, Deep Fashion3D [24] uses an implicit Occupancy Network [57] to model fine geometric details on garment surfaces. Zhu *et al.* [26] extend this idea by proposing a novel geometry inference network ReEF, which registers an explicit garment template to a pixel-aligned implicit field through progressive stages including template initialization, boundary alignment and shape fitting. Zhao *et al.* [53] utilize the predicted 3D anchor points to learn an unsigned distance function, which enables the handling of open garment surfaces with complex topology. However, these methods cannot deal with dynamic clothing, thus they are not suitable for dynamic garment reconstruction.

Other methods [9], [58]–[61] try to reconstruct dynamic clothing from video. Garment Avatar [58] proposes a multi-view patterned clothing tracking algorithm capable of capturing deformations with high accuracy. Li *et al.* [9] propose a method for learning physically-aware clothing deformations from monocular videos, but their method relies on an individual-dependent 3D template mesh [59]. SCARF [60] combines the strengths of body mesh models (SMPL-X [62]) with the flexibility of NeRFs [45], but the geometry of clothing is sometimes noisy due to the limited 3D geometry quality for NeRF reconstruction. REC-MV [61] introduces a method to jointly optimize the explicit feature curves and the implicit signed distance field (SDF) of the garments to produce high-quality dynamic garment surfaces. These solutions show their strength in reconstructing high-fidelity layered representations

with garments that remain in consensus with the input person. However, this design leaves out the body pose, which makes it impossible to control or animate garments flexibly.

In this paper, we design a weakly supervised framework to recover high-quality dynamic garments from a monocular video without depending on scanned data. In the meanwhile, we propose a learnable garment deformation network which enables our model to generate reasonable deformations for various unseen poses.

### III. METHOD

Our goal is to reconstruct high-quality animatable dynamic garments from a monocular video, which effectively enables personalized clothing animation. Previous works not only rely on expensive data, but are also bounded by domain gaps and cannot generalize well to inputs outside the domain of the training dataset. Therefore, we propose to reconstruct clothes in a weakly supervised manner, thus addressing the main drawbacks of previous works in terms of cost. Given a monocular video which consists of a clothed human under random poses, we first extract human-centric information such as segmentation maps and normal maps [63]–[66] to help obtain consistent geometry details with the input video (Sec. III-A). To enable the generation of animatable dynamic garments for various unseen poses, we propose a learnable garment deformation network based on human body priors which formulates the garment reconstruction task as a pose-driven deformation problem (Sec. III-B). In addition, different from previous works which estimate a unique displacement vector for each garment vertex, our method leverages a multi-hypothesis deformation module to alleviate the depth ambiguity and provide integrated deformations for the final reconstructed garments (Sec. III-C). The overview of our method is illustrated in Fig. 2.

#### A. Human-Centric Information Extracting

To get rid of costly data preparation, we design a weakly supervised framework to recover high-quality dynamic garments from monocular videos, and we extract human-centric information which is helpful to obtain consistent geometry details with the input. Specifically, given a monocular video  $I = \{\mathbf{I}_0, \dots, \mathbf{I}_{n-1}\}$ , where  $n$  is the number of frames, we first use a state-of-the-art human pose estimation method [67] to estimate the pose parameters  $\theta \in \mathbb{R}^{72}$  and the shape parameters  $\beta \in \mathbb{R}^{10}$  of a SMPL human body model [27], as well as the weak-perspective camera parameters  $c \in \mathbb{R}^3$  for each frame. The pose parameters  $\theta$  and the shape parameters  $\beta$  represent 3D rotations of human body joints and PCA (Principal Component Analysis) coefficients of T-posed body shape space, respectively. Second, we obtain the binary masks  $\mathbf{Ms} = \{\mathbf{Ms}_0, \dots, \mathbf{Ms}_{n-1}\}$  of the input  $I$  using a robust human parsing method PGN [68]. Note that the output of PGN is a set of segmentation masks, where each pixel corresponds to a human body part or clothing type. We remove the masks of the human body, leaving only the ones of the clothing, and transform segmentation masks to binary masks. Third, we use PIFuHD [37] to estimate the image normals

$\mathbf{Nor} = \{\mathbf{Nor}_0, \dots, \mathbf{Nor}_{n-1}\}$  of the input  $I$  and multiply them by the binary masks  $\mathbf{S}$  to get the normal map of the garment. Finally, we obtain the smooth garment template  $\mathbf{T}$  of the first frame under T-pose based on the work of Jiang *et al.* [23]. The information above helps reduce the complexity inherent to our garment reconstruction. Our template supports six garment categories, including upper garment, pants, and skirts with short and long templates for each type.

#### B. Garment Deformation Network

The absence of strong and efficient human priors increases the difficulty of estimating dynamic and reasonably wrinkled clothing directly from a monocular video. Different from previous works which extract features from images to generate clothing deformations, we observe that the garment deformation is caused by changes in pose. Therefore, we design a garment deformation network which enables our model to generate reasonable deformations for various unseen poses. To achieve this, we use a parametric SMPL model [27] to guide the deformation of the spatial points of garments [69], which enables explicit transformation from template space to current posed space. With the SMPL model, we can map the shape parameters  $\beta$  and the pose parameters  $\theta$  to a body mesh  $\mathbf{M}_b$ . The mapping can be summarized as:

$$\begin{aligned} \mathbf{M}_b(\beta, \theta) &= W_b(\mathbf{T}_b(\beta, \theta), \mathbf{J}(\beta), \theta, \mathcal{W}_b), \\ \mathbf{T}_b(\beta, \theta) &= \mathbf{B} + \mathbf{B}_s(\beta) + \mathbf{B}_p(\theta), \end{aligned} \quad (1)$$

where  $W_b$  is the linear blend skinning function of the human body,  $\mathbf{J}(\beta)$  is the SMPL body's skeleton, and  $\mathcal{W}_b$  is the blend weights of each vertex of SMPL.  $\mathbf{B}_s(\beta)$  and  $\mathbf{B}_p(\theta)$  are the pose blendshape and shape blendshape, respectively. As most clothes follow the deformation of the body, we share garment pose parameters  $\theta$  with SMPL and use SMPL's skeleton  $\mathbf{J}(\beta)$  as the binding skeleton of the garment. In this way, we define our cloth mesh  $M_c$  as follows:

$$\begin{aligned} \mathbf{M}_c(\beta, \theta) &= W_c(\mathbf{T}_c(\theta), \mathbf{J}(\beta), \theta, \mathcal{W}_c), \\ \mathbf{T}_c(\theta) &= \mathbf{T} + D_\theta, \end{aligned} \quad (2)$$

where  $W_c$  is the linear blend skinning function of the garment,  $\mathcal{W}_c$  is the blend weights of each vertex of the garment,  $\mathbf{T}$  is the smooth garment template and  $D_\theta$  is the high-frequency displacement over the garment template.

For the pose  $\theta$  of each frame, we design a four-layer Multi-Layer Perceptron (MLP) with ReLU activation function to obtain a high-level embedding  $X$ , and further obtain the garment vertex deformations  $D_\theta$  with a learnable matrix  $G \in \mathbb{R}^{x \times N \times 3}$  (where  $x$  is the dimensionality of the high-level embedding and  $N$  is the number of vertices of the garment mesh). This non-linear mapping from  $\theta$  to  $D_\theta$  allows modeling high-frequency details, such as wrinkles caused by different poses, which are beyond the representation ability of the linear model. For each vertex on the garment template, instead of directly using the skinning weights of SMPL, we assign its blend weights equal to those of the closest body vertex and allow the blend weights to be optimized during training to make the garment mesh independent from the SMPL. Our garment deformation network can reconstruct

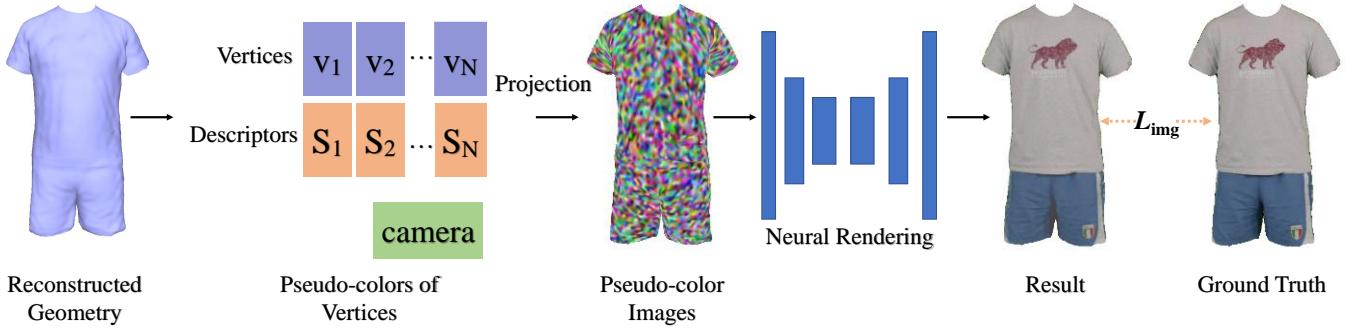


Fig. 3. An overview of our neural rendering pipeline. Given the reconstructed mesh with the descriptors and the camera, we first project the mesh onto the image plane, using descriptors as pseudo-colors. We then use the rendering network to transform the pseudo-color images into a photo-realistic RGB image.

pose-dependent garments, which enables the generation of reasonable deformations for various unseen poses.

### C. Multi-Hypothesis Displacement

Recovering 3D clothes from monocular videos is a highly uncertain and inherently ill-posed problem. We propose a multi-hypothesis displacement module that learns spatial representations of multiple plausible deformations in the learnable garment deformation network. Since each pixel of the image corresponds to innumerable points in the 3D space, it is difficult to specify a unique 3D point corresponding to a given pixel. To alleviate the depth ambiguity brought by estimating 3D garments from monocular video, different from previous works which estimate a unique displacement vector for each garment vertex, we design a cascaded architecture to generate multiple displacements using the high-level pose embedding  $X$ . More specifically, we first define three learnable matrices to get three deformations and encourage gradient propagation through residual connections. Then, we connect the three hypothetical deformations as the input of an MLP that outputs the final deformation. These procedures can be formulated as:

$$\begin{aligned}
 X &= \sigma(\mathcal{F}_{\text{MLP}_1}(\theta)), \\
 D_1 &= \sigma(X \cdot G_1 + b_1), \\
 D_2 &= \sigma(D_1 + X \cdot G_2 + b_2), \\
 D_3 &= \sigma(D_2 + X \cdot G_3 + b_3), \\
 D_\theta &= \mathcal{F}_{\text{MLP}_2}(D_1, D_2, D_3),
 \end{aligned} \tag{3}$$

where  $X$  is the high-level embedding mentioned in Sec. III-B,  $\sigma$  denotes the ReLU activation function,  $G_*$  and  $b_*$  are the learnable matrices and bias terms respectively, and  $\mathcal{F}_{\text{MLP}_*}$  represents Multi-Layer Perceptron. For simplicity, we use  $*$  to represent an arbitrary subscript. With this design, our model can first predict multiple displacements, which can enrich the diversity of features, and then aggregate them to produce more reasonable displacements for the 3D garments. Finally, these displacements are added to the garment template to obtain the result in T-pose, which is then skinned along the body according to pose parameters  $\theta$  and blend weights  $\mathcal{W}_c$  to produce the final result.

### D. Loss Function

The loss function of our weakly supervised network includes the constraints from the image and the geometric constraints of the clothes, which not only produces image-consistent details, but also keeps the garment stable. The overall loss function is

$$L = L_{\text{img}} + L_{\text{cloth}}. \tag{4}$$

• **Image Loss.** To generate garment geometry and shape that are consistent with the input, we regularize the shape of clothing by projecting it onto an image, and compute the loss with the target mask  $S_i$  and we utilize the predicted normal map to further refine the geometry shape. We define the following image loss:

$$\begin{aligned}
 L_{\text{img}} &= \lambda_{\text{mask}} \|\mathcal{F}_{\text{mask}}(M_i, c) - \mathbf{M}\mathbf{s}_i\|_2 \\
 &+ \lambda_{\text{normal}} \|\mathcal{F}_{\text{VGG}}(\mathcal{F}_{\text{normal}}(M_i, c)) - \mathcal{F}_{\text{VGG}}(\mathbf{M}\mathbf{s}_i \cdot \mathbf{Nor}_i)\|_2,
 \end{aligned} \tag{5}$$

where  $\lambda_{\text{mask}}$  and  $\lambda_{\text{normal}}$  are the weights that balance the contributions of individual loss terms.  $\mathcal{F}_{\text{mask}}$  is a differentiable renderer [70] that renders the mask of garment mesh  $M_i$  corresponding to the  $i$ -th frame, given the camera parameters  $c$ .  $\mathcal{F}_{\text{normal}}$  outputs the normal map in a similar way to  $\mathcal{F}_{\text{mask}}$ ,  $\mathbf{M}\mathbf{s}_i \cdot \mathbf{Nor}_i$  is the normal map of the garment as mentioned in Sec. III-A, and  $\mathcal{F}_{\text{VGG}}$  is the VGG-16 network used to extract image features to help measure their similarity.

• **Clothing Loss.** Using only the image loss is inclined to produce unstable results. Thus another clothing loss term is added to enhance stability of the reconstructed garments:

$$\begin{aligned}
 L_{\text{cloth}} &= \lambda_{\text{edge}} \|E - E_T\|_2^2 + \lambda_{\text{face}} \|\Delta(N_F)\|_2^2 \\
 &+ \lambda_{\text{angle}} \|\Theta\|_2^2 + \lambda_{\text{collision}} \sum_{j=0}^{V_b} \max(\varepsilon - d_j \cdot n_j, 0)^2.
 \end{aligned} \tag{6}$$

$E$  is the predicted edge lengths,  $E_T$  is the edge lengths on the template garment  $\mathbf{T}$ ,  $N_F$  is the face normals,  $\Delta(\cdot)$  is the Laplace-Beltrami operator, and  $\Theta$  is the dihedral angle between faces.  $\lambda_{\text{edge}}$ ,  $\lambda_{\text{face}}$ ,  $\lambda_{\text{angle}}$  and  $\lambda_{\text{collision}}$  are the balancing weights. where  $d_j$  is the vector going from the  $j$ -th vertex of the body vertices  $V_b$  to the nearest vertex of the garment,  $n_j$  is the normal of the  $j$ -th body vertex,  $\varepsilon$  is a small positive threshold. On the one hand, inspired by [71], [72], the first

three terms of  $L_{\text{cloth}}$  ensure the clothing is not excessively stretched or compressed and enforces locally smooth surfaces. On the other hand, the last item of  $L_{\text{cloth}}$  is used to handle the collision between the clothes and the body.

### E. Implementation Details

Our model is implemented using Tensorflow, and we train our model for 10 epochs with a batch size of 8 using the Adam optimizer [73] with a learning rate of  $1 \times 10^{-4}$ . The embedding dimensions of the MLP used to obtain the high-level embedding are set to 256, 256, 512 and 512, respectively, and the learnable matrix is initialized using the truncated normal distribution. We choose the weights of the individual losses with  $\lambda_{\text{mask}} = 500$ ,  $\lambda_{\text{normal}} = 1500$ ,  $\lambda_{\text{edge}} = 100$ ,  $\lambda_{\text{face}} = 2000$ ,  $\lambda_{\text{angle}} = 1$  and  $\lambda_{\text{collision}} = 100$ . For a video of about 600 frames in length with a resolution of  $512 \times 512$ , we train our model with a Titan X GPU in half an hour.

## IV. NEURAL TEXTURE GENERATION

The prior works [22], [23], [25] focus on the geometry of the clothes and do not attempt to recover the garment textures, which limits the application scenarios. Texture is extremely complex: it resides in high-dimensional space and is difficult to represent. Therefore, to cope with the complexity of textures, we propose a neural texture network to obtain photo-realistic results. As different garment meshes have different topologies, it is computationally expensive to generate a UV map every time. Inspired by [75], [76], our main idea is to combine the point-based graphics and neural rendering. Below, we will explain the details of our method. An overview of our neural rendering pipeline is illustrated in Figure 3.

Based on the multi-hypothesis displacement module, we get the relatively accurate geometry of clothing mesh  $M_c$ , which allows the neural texture network to focus on texture information. We first attach descriptors  $S = \{S_1, \dots, S_N\}$  which serve as pseudo-colors, to the garment mesh vertices  $V = \{V_1, \dots, V_N\}$ . We first project the mesh onto the image plane to obtain pseudo-color image  $R_{img}$ , then use the neural texture network to transform the pseudo-color image  $R_{img}$  into a photo-realistic RGB image  $I_{img}$ . Specifically, given the pseudo-color image and the ground truth image, we adopt a UNet-based neural texture network to map the initial mesh projections to the final output image. The neural texture network consists of 8 blocks of downsampling and 8 blocks of upsampling convolutional layers. Each downsampling block consists of a convolution layer with BatchNorm operations followed by ReLU activations; each upsampling block consists of a transposed convolution layer with BatchNorm operations followed by ReLU activations.

Using the ground-truth image  $I_{gt}$ , we optimize our neural texture network by minimizing the differences between the rendered image  $I_{img}$  and ground-truth RGB image  $I_{gt}$ . to obtain higher quality results, we adopt a two-stage training strategy. In the first stage, we optimize the descriptor to obtain a better initial value for the second stage. Specifically, during the first stage, we train the model using the Adam optimizer with a learning rate of  $1 \times 10^{-4}$  and the batch size of 4 for

25 epochs by minimizing the perceptual loss between pseudo-color image and ground-truth image:

$$L_{\text{pse}} = \|\mathcal{F}_{\text{VGG}}(R_{img}) - \mathcal{F}_{\text{VGG}}(I_{gt})\|_2, \quad (7)$$

where  $\mathcal{F}_{\text{VGG}}$  is the image features extracted from the VGG-16 network which is used to ensure the perceptual similarity.

During the second stage, we train the model for 25 epochs using the Adam optimizer with a learning rate of  $1 \times 10^{-4}$  which is decayed by a factor of 0.5 every 10 epochs:

$$L_{\text{render}} = \|\mathcal{F}_{\text{VGG}}(I_{gt}) - \mathcal{F}_{\text{VGG}}(I_{img})\|_2 + \lambda_{\text{render}} \|I_{gt} - I_{img}\|_1, \quad (8)$$

where  $\lambda_{\text{render}}$  is the balancing weight and is set to 100 in our experiments. The overall training time is around 1.5 hours with a Titan X GPU.

## V. EXPERIMENTS

### A. Datasets

To demonstrate the effectiveness of our proposed method, we conduct experiments on four different datasets: People-Snapshot [18], CAPE [74], IPER [77] and our captured data. People-Snapshot [18], IPER and our captured data contain different monocular RGB videos captured in real-world scenes, where subjects turn around with a rough A-pose in front of an RGB camera. In addition, IPER and our captured data also contain videos of the same person with random motions. CAPE [74] is a dynamic dataset of clothed humans which provides raw scans of 4 subjects performing simple motions. These four datasets are used to evaluate the quality of the 3D reconstructions, IPER and our captured data are also used to show the results of garment animation. The SMPL parameters provided by CAPE [74] and People-Snapshot [18] are used. For the input video, 80% is used for training (Reconstruction) and 20% is used for testing (Animation).

### B. Comparison

We compare our method against the state-of-the-art garment reconstruction methods that release the codes: Multi-Garment Net (MGN) [22], BCNet [23], and SMPLicit [25], both qualitatively and quantitatively. Note that these methods all apply supervised learning, either using 3D scans or synthetic datasets to train the models, while we propose to reconstruct clothes in a weakly supervised manner without 3D supervision.

TABLE I  
QUANTITATIVE COMPARISON ON CAPE DATASET.

Method	00032		00096		00159		03223	
	CD↓	CCV↓	CD↓	CCV↓	CD↓	CCV↓	CD↓	CCV↓
SMPLicit	1.611	-	1.866	-	1.811	-	1.599	-
MGN	1.328	2.927	1.850	2.055	1.345	2.959	1.452	2.983
BCNet	1.591	3.877	1.240	4.212	1.270	2.305	1.477	2.350
Ours	<b>1.098</b>	<b>1.819</b>	<b>1.049</b>	<b>1.217</b>	<b>1.087</b>	<b>0.961</b>	<b>1.072</b>	<b>0.713</b>

**Qualitative Comparison.** In Fig. 4, we show the visual results of the same person in three different poses. It can be seen that for different poses, our reconstruction method produces

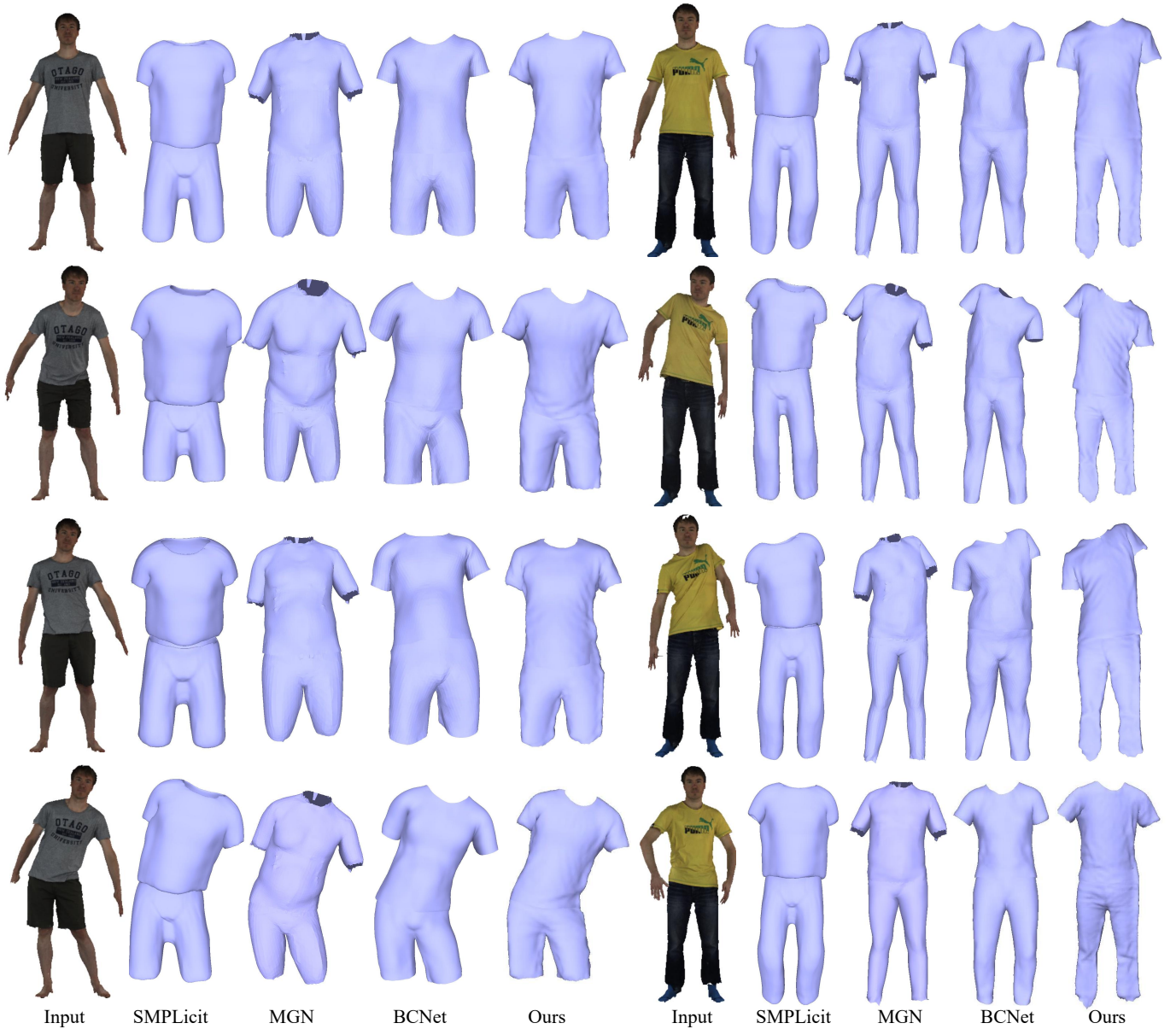


Fig. 4. Reconstructed garments by SMPLicit [25], MGN [22], BCNet [23] and our method on CAPE dataset [74]. The inputs are four frames of a motion sequence.

TABLE II  
QUANTITATIVE EVALUATION FOR MULTI-HYPOTHESIS DISPLACEMENT  
MODULE ABLATION STUDY (CM).

Method	00032		00096		00159		03223	
	CD↓	CCV↓	CD↓	CCV↓	CD↓	CCV↓	CD↓	CCV↓
w/o MHD	1.167	1.835	1.130	1.204	1.198	1.076	1.159	0.743
MHD2	1.105	1.828	1.051	1.203	1.090	0.968	1.079	0.719
MHD3	<b>1.098</b>	<b>1.819</b>	<b>1.049</b>	1.217	1.087	0.961	<b>1.072</b>	<b>0.713</b>
MHD4	1.110	1.829	1.059	<b>1.193</b>	1.087	0.972	1.086	0.718
MHD5	1.106	1.820	1.057	1.194	<b>1.083</b>	<b>0.960</b>	1.089	0.720
MHD6	1.105	1.828	1.056	1.206	1.089	0.961	1.085	0.718

TABLE III  
QUANTITATIVE EVALUATION FOR LOSS FUNCTION ABLATION STUDY  
(CM).

Method	00032		00096		00159		03223	
	CD↓	CCV↓	CD↓	CCV↓	CD↓	CCV↓	CD↓	CCV↓
w/o Cloth Loss	1.397	1.844	1.552	1.243	1.677	<b>0.924</b>	1.580	0.725
w/o Image Loss	1.172	<b>1.808</b>	1.128	1.275	1.174	0.967	1.158	0.781
Full	<b>1.098</b>	1.819	<b>1.049</b>	<b>1.217</b>	<b>1.087</b>	0.961	<b>1.072</b>	<b>0.713</b>

different deformations consistent with the image, while MGN [22] and SMPLicit [25] can only produce smooth results. BCNet [23] can generate some details, but not as rich as

ours. In Fig. 5, since the person maintains a rough A-pose during rotation, we only show the results of the first frame of the video. It can be seen that MGN [22] and SMPLicit [25] cannot get accurate clothing styles. While BCNet [23] can get visually reasonable shapes, it cannot produce geometric

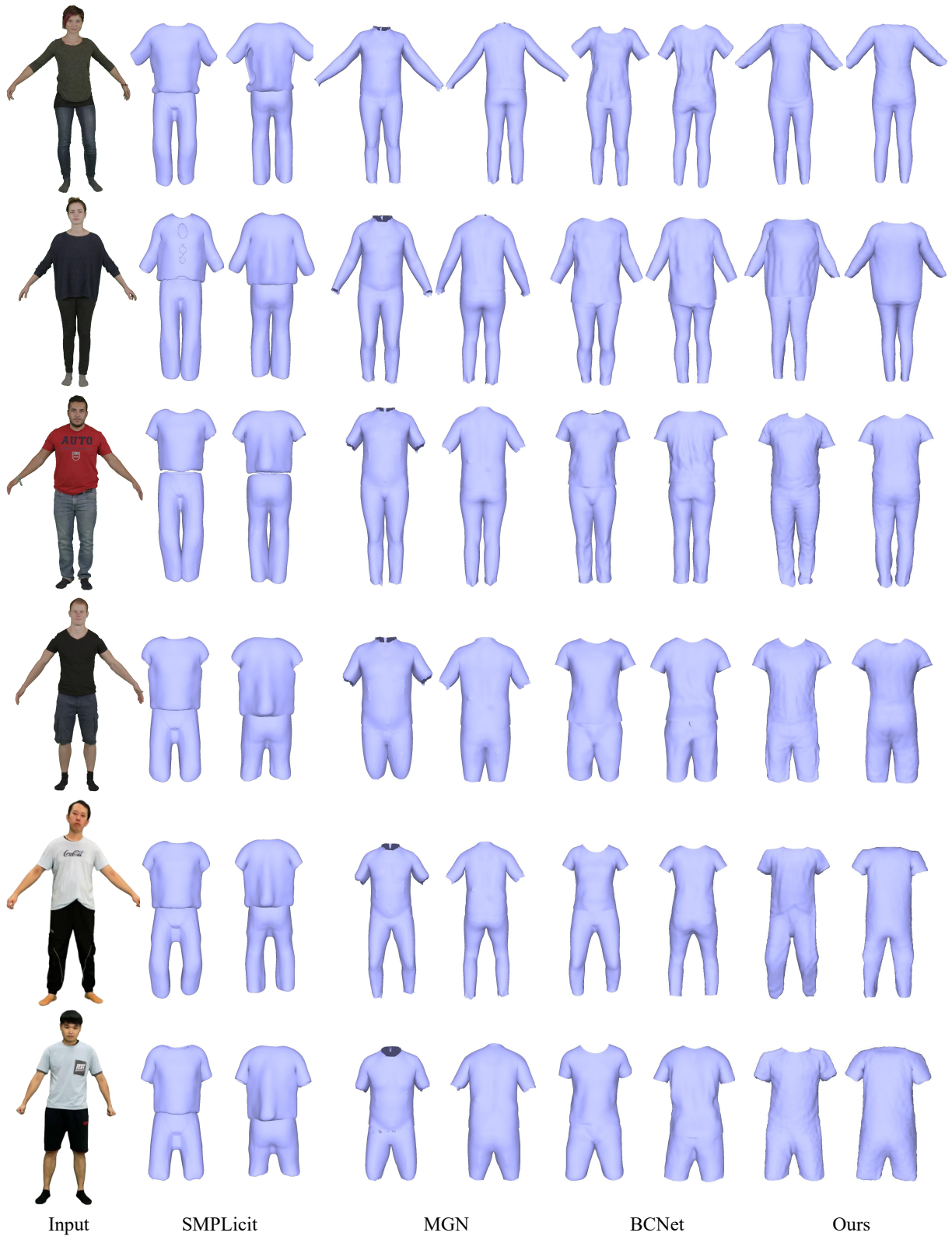


Fig. 5. Reconstructed garments by SMPLicit [25], MGN [22], BCNet [23] and our method on People-Snapshot [18] dataset (top four rows) and our captured data (bottom two rows).

details that are consistent with the input, or even produces wrong details. On the contrary, our approach benefits from the weakly supervised framework and reconstructs high-quality

garments which faithfully reflect the input appearances. The elegant design of the multi-hypothesis displacement module also enables back surfaces with reasonable details to be gener-

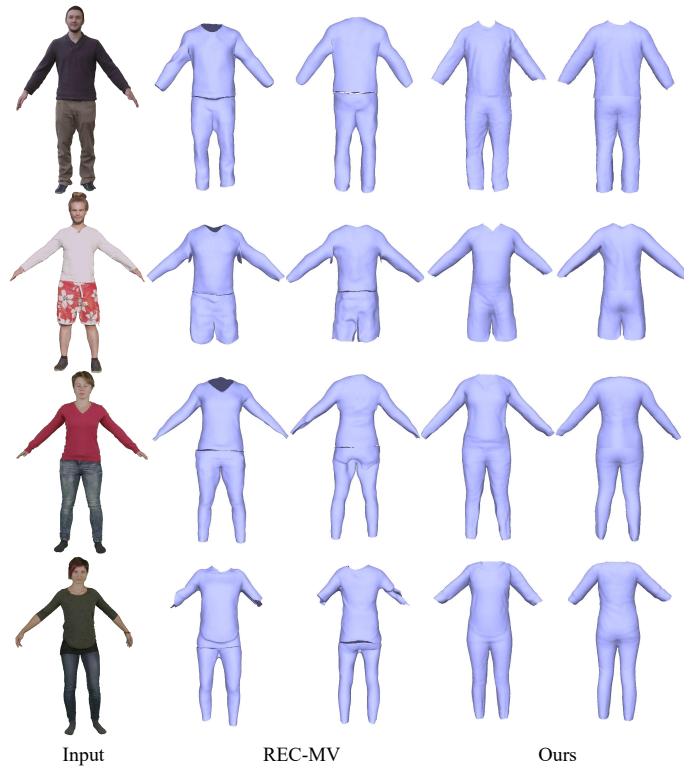


Fig. 6. Reconstructed garments by REC-MV [61] and our method on People-Snapshot [18] dataset.

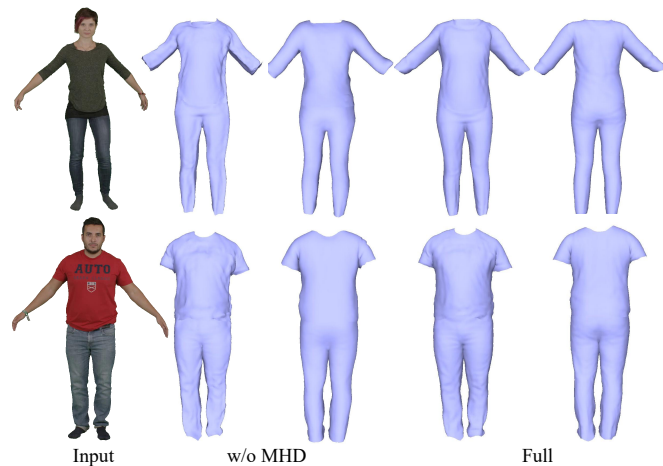


Fig. 7. Qualitative results of multi-hypothesis displacement module ablation study.

ated, given the input of the front view. To further demonstrate the effect of our model, we also compare our method with a video-based method REC-MV [61]. In the current REC-MV source code, there is an absence of data preprocessing code, *e.g.*, estimating the feature lines of the clothes from the input, which is based on their previous work called Deep Fashion3D [24] and is currently not accessible. Therefore, we can only make a qualitative comparison on the People-Snapshot dataset, because the preprocessing data of the People-Snapshot dataset is released. In Fig. 6, since the person maintains a rough A-pose during rotation, we only show the results of the first

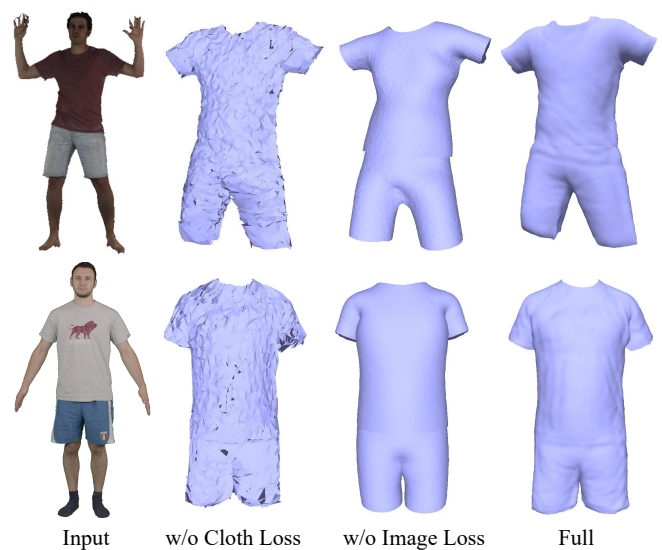


Fig. 8. Qualitative results of loss function ablation study.



Fig. 9. Qualitative results of garment template ablation study.

frame of the video. It can be seen that our model can not only reconstruct the garment geometry consistent with the image, but also keep the garment stable. Compared to our method, the training time of REC-MV is around 18 hours with an RTX 3090 GPU, while we train our model with a TITAN X GPU in half an hour. Besides, the results of REC-MV could not be animated. More dynamic results can be found in supplementary video.

**Quantitative Comparison.** We test our method and the state-of-the-art methods with the rendered images from CAPE [74] dataset. Note that we use all the subjects with raw scans ('00032-shortshort-hips', '00096-shortshort-tilt-twist-

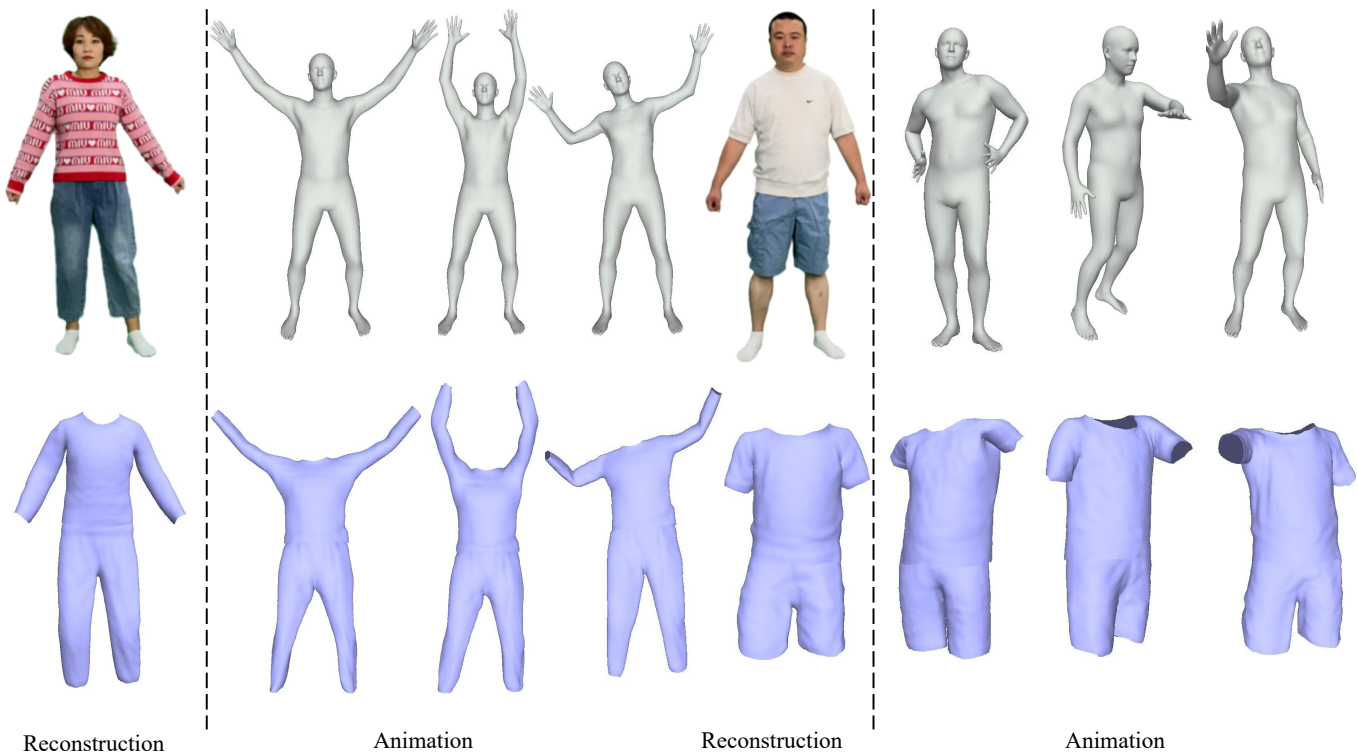


Fig. 10. Garment animation results.

TABLE IV

QUANTITATIVE EVALUATION FOR GARMENT TEMPLATE ABLATION STUDY (CM).

Method	00032		00096		00159		03223	
	CD↓	CCV↓	CD↓	CCV↓	CD↓	CCV↓	CD↓	CCV↓
Ours-MGN	1.246	1.896	1.078	<b>0.968</b>	1.135	1.039	1.201	0.979
Full	<b>1.098</b>	<b>1.819</b>	<b>1.049</b>	1.217	<b>1.087</b>	<b>0.961</b>	<b>1.072</b>	<b>0.713</b>

TABLE V

QUANTITATIVE EVALUATION FOR GARMENT ANIMATION (CM).

Method	00032		00096		00159		03223	
	CD↓	CCV↓	CD↓	CCV↓	CD↓	CCV↓	CD↓	CCV↓
reconstruction	<b>1.098</b>	<b>1.819</b>	<b>1.049</b>	<b>1.217</b>	<b>1.087</b>	<b>0.961</b>	<b>1.072</b>	<b>0.713</b>
animation	1.103	2.543	1.081	2.065	1.097	1.076	1.112	0.743

left’, ‘00159-shortlong-pose-model’, ‘03223-shortlong-hips’) from CAPE [74] dataset, and for brevity, only the ID of the subject is kept in the table in the rest of this section. We first align the garment meshes generated by different methods to the ground truth meshes across all frames for a video and then compute the the final average Chamfer distance between the reconstructed garments and the ground truth meshes for accuracy measurement. To evaluate the temporal consistency of the reconstructed meshes, we measure the consistency of corresponding vertices (CCV), which is the root mean squared error of the corresponding vertices’ distances in adjacent frames. As shown in Table I, our method outperforms other methods in reconstruction accuracy, which indicates more realistic reconstruction results from a single RGB camera.

### C. Ablation Study

**Multi-Hypothesis Displacement.** To validate the effect of the multi-hypothesis displacement module, we compare the performances of using different numbers of hypotheses. Specifically, given the high-level embedding of the pose, we define different numbers of learnable matrices to get deformations and encourage gradient propagation through residual connections. Then, we connect these hypothetical deformations as the input of an MLP to output the final deformation. Table II gives the quantitative results on CAPE dataset [74]. We calculate the average Chamfer distance between the aligned reconstructed garments and the ground truth meshes across all frames for a video and consistency of corresponding vertices (CCV) between adjacent frames. As shown in Table II, different numbers of hypotheses achieve similar accuracies, and all have higher accuracies than w/o MHD. In the rest of this section, we utilize MHD3 as our full model. Some visual results are shown in Fig. 7. It can be seen that our full model addresses the problems faced by w/o MHD, such as messy details and over-smooth back surfaces. At the same time, it also proves the effectiveness of our multi-hypothesis module, which can learn the dynamic deformations of clothes well from monocular video.

**Loss Function.** We study the effects of different loss functions on garment reconstruction. Our method is compared with two variants: one supervised without clothing loss function (w/o Cloth Loss), and the other supervised without image loss function (w/o Image Loss). In the same way as before, we calculate the average Chamfer distance between the aligned reconstructed garments and the ground truth meshes across



Fig. 11. Neural texture generation by our method on Cape dataset (left three columns) and People-Snapshot dataset (right three columns).

all frames for a video ywand consistency of corresponding vertices (CCV) between adjacent frames. Table III gives the quantitative results in terms of the Chamfer distance and consistency of corresponding vertices (CCV). Our full model achieves the best performance, which verifies the importance of adopting both the image loss and the clothing loss. As shown in Fig. 8, the variant without the clothing loss generates messy meshes, while the variant without the image loss generates smooth meshes. In contrast, our full model can not only reconstruct the garment geometry consistent with the image, but also keep the garment stable.

**Garment Template.** We study the effects of different parametric garment templates on garment reconstruction. We compare our method with a variant template generated by MGN (Ours-MGN). In the same way as before, we calculate the average Chamfer distance between the aligned reconstructed garments and the ground truth meshes across all frames for a video and consistency of corresponding vertices (CCV) between adjacent frames. Table IV gives the quantitative results in terms of the Chamfer distance and consistency of corresponding vertices (CCV). Our full model achieves slightly better performance than Ours-MGN. Both Ours-MGN and our full model out-

perform other state-of-the-art (SOTA) methods. As shown in Fig. 9, Ours-MGN also reconstructs the garment geometry consistent with the image, but at the neckline and cuffs, there are a lot of messy triangle faces.

#### D. Garment Animation

We utilize a parametric body model of SMPL [27] which makes the garment deformation more controllable, in order to handle dynamic garment reconstruction from monocular videos. Thanks to the design of the learnable garment deformation network, our method can generate reasonable deformations for unseen poses. Specifically, we train the model using our captured videos and test it with random unseen pose sequences. Table V gives the quantitative results in terms of the Chamfer distance, as well as the consistency of corresponding vertices (CCV) between adjacent frames. As shown in the Table V, our method achieves similar accuracy on unseen poses. Figure 10 shows that our method can still produce garments with well-preserved personal identity and clothing details of the subjects under various novel poses, which enables dynamic garment animation. More dynamic results can be found in supplementary video.

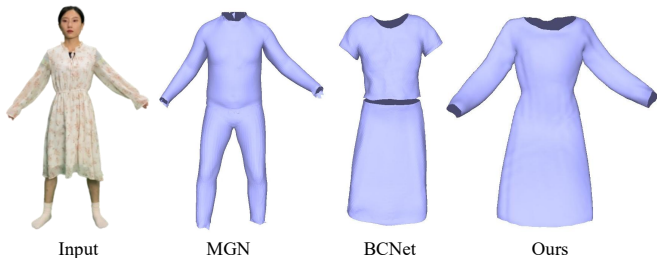


Fig. 12. Reconstructed loose garment by MGN [22], BCNet [23] and our method on our captured data.

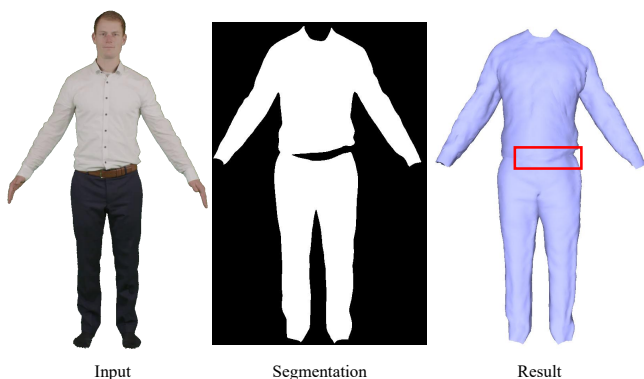


Fig. 13. An example of imprecisely reconstructed clothing due to wrong segmentation result.

#### E. Texture Generation

Figure 11 shows some qualitative results by our neural texture generation method. As shown in the figure, our method can not only obtain high-quality garment geometry, but also produce high-fidelity textures consistent with the image. More dynamic results can be found in the supplementary video.

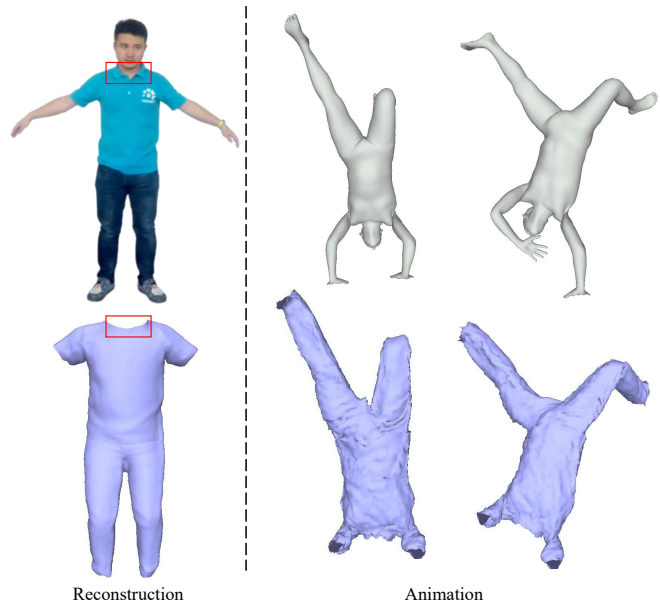


Fig. 14. Examples of failure cases for collars and extreme poses.

#### F. Discussion and Limitations

Although we have achieved high-quality animatable dynamic garment reconstruction from a single RGB camera, there are still some cases that we cannot solve well:

**Loose Clothing.** The results of cases with loose clothes may not be good, due to less relevance between body and clothing. Figure 12 shows some comparison results. Our method can obtain visually reasonable clothing shapes, but cannot recover folded structures consistent with the image. In further work, we will design a temporal fusion module that uses information from adjacent frames to improve the representation of the framework and generate higher quality animatable dynamic garments.

**Collars.** While our method can reconstruct garment meshes with high-quality surface details from a monocular video, it fails to reconstruct collars due to the lack of supervision of the collars. Fig. 14 gives some examples of such cases. We will explore a post-processing to extend our method to address this.

**Extreme Poses.** Although our method can generate reasonable deformations for unseen poses, it may produce incorrect results for extreme poses. Fig. 14 gives some examples of extreme poses cases. This could be solved by adding garment priors and training with more poses in the future work.

**Segmentation and Normal Estimation.** By applying weakly supervised training, we eliminate the need to simulate or scan hundreds or even thousands of sequences. Instead, our method uses predicted clothing segmentation masks and normal maps as the 2D supervision during training. The errors of segmentation and normal estimation could have negative effects on the training process and lead to imprecise reconstruction. Fig. 13 gives some examples of wrong clothing segmentation.

## VI. CONCLUSION

In this paper, we aim to solve a meaningful but challenging problem: reconstructing high-quality animatable dynamic garments from monocular videos. We propose a weakly supervised framework to eliminate the need to simulate or scan hundreds or even thousands of sequences. To the best of our knowledge, no other work meets the expectations of digitizing high-quality garments that can be adjusted to various unseen poses. In particular, we propose a learnable garment deformation network that formulates the garment reconstruction task as a pose-driven deformation problem. This design enables our model to generate reasonable deformations for various unseen poses. To alleviate the ambiguity brought by estimating 3D garments from monocular videos, we design a multi-hypothesis deformation module that learns spatial representations of multiple plausible deformation hypotheses. In this way, we can alleviate the ambiguity brought by estimating 3D garments based on monocular videos. The prior works [22], [23], [25] focus on the geometry of the clothes and do not attempt to recover the garment textures, which limits their application scenarios. Therefore, we design a neural texture network to generate high-fidelity textures consistent with the image. Experimental results on several public datasets demonstrate that our method can reconstruct high-quality dynamic garments with coherent surface details, which can be easily animated under unseen poses.

## REFERENCES

- [1] Y. Fu, R. Li, T. S. Huang, and M. Danielsen, "Real-time multimodal human-avator interaction," *IEEE Trans. Circuit Syst. Video Technol.*, pp. 467–477, 2008.
- [2] J. Yang, X. Guo, K. Li, M. Wang, Y.-K. Lai, and F. Wu, "Spatio-temporal reconstruction for 3D motion recovery," *IEEE Trans. Circuit Syst. Video Technol.*, pp. 1583–1596, 2020.
- [3] N. Jovic, J. Gu, T. Shen, and T. S. Huang, "Computer modeling, analysis, and synthesis of dressed humans," *IEEE Trans. Circuit Syst. Video Technol.*, pp. 378–388, 1999.
- [4] O. Sarakatsanos, E. Chatzilari, S. Nikolopoulos, I. Kompatsiaris, D. Shin, D. Gavilan, and J. Downing, "A VR application for the virtual fitting of fashion garments on avatars," in *Proc. IEEE International Symposium on Mixed and Augmented Reality*, 2021, pp. 40–45.
- [5] A. C. S. Genay, A. Lécuyer, and M. Hachet, "Being an avator "for Real": A survey on virtual embodiment in augmented reality," *IEEE Trans. Vis. Comput. Graph.*, pp. 1–27, 2021.
- [6] S. Pujades, B. Mohler, A. Thaler, J. Tesch, N. Mahmood, N. Hesse, H. H. Bühlhoff, and M. J. Black, "The Virtual Caliper: Rapid creation of metrically accurate avatars from 3D measurements," *IEEE Trans. Vis. Comput. Graph.*, pp. 1887–1897, 2019.
- [7] Y. Xu, S. Yang, W. Sun, L. Tan, K. Li, and H. Zhou, "3D virtual garment modeling from RGB images," in *Proc. IEEE International Symposium on Mixed and Augmented Reality*, 2019, pp. 37–45.
- [8] X. Li, J. Huang, J. Zhang, X. Sun, H. Xuan, Y.-K. Lai, Y. Xie, J. Yang, and K. Li, "Learning to infer inner-body under clothing from monocular video," *IEEE Trans. Vis. Comput. Graph.*, pp. 1–14, 2022.
- [9] Y. Li, M. Habermann, B. Thomaszewski, S. Coros, T. Beeler, and C. Theobalt, "Deep physics-aware inference of cloth deformation for monocular human performance capture," in *Int. Conf. on 3D Vis.* IEEE, 2021, pp. 373–384.
- [10] C. Zhang, S. Pujades, M. J. Black, and G. Pons-Moll, "Detailed, accurate, human shape estimation from clothed 3D scan sequences," in *IEEE Conf. Comput. Vis. Pattern Recog.*, 2017, pp. 4191–4200.
- [11] X. Chen, A. Pang, W. Yang, P. Wang, L. Xu, and J. Yu, "TightCap: 3D human shape capture with clothing tightness field," *ACM Trans. Graph.*, vol. 41, pp. 1–17, 2021.
- [12] Z. Lahner, D. Cremers, and T. Tung, "DeepWrinkles: Accurate and realistic clothing modeling," in *Eur. Conf. Comput. Vis.*, 2018, pp. 667–684.
- [13] K. Li, J. Yang, L. Liu, R. Boulic, Y.-K. Lai, Y. Liu, Y. Li, and E. Molla, "Spa: Sparse photorealistic animation using a single RGB-D camera," *IEEE Trans. Circuit Syst. Video Technol.*, pp. 771–783, 2017.
- [14] D. S. Alexiadis, A. Chatzitofis, N. Zioulis, O. Zoidi, G. Louizis, D. Zarpalas, and P. Daras, "An integrated platform for live 3D human reconstruction and motion capturing," *IEEE Trans. Circuit Syst. Video Technol.*, pp. 798–813, 2017.
- [15] P. Cong, Z. Xiong, Y. Zhang, S. Zhao, and F. Wu, "Accurate dynamic 3D sensing with fourier-assisted phase shifting," *IEEE J. Sel. Top. Sign. Process.*, pp. 396–408, 2015.
- [16] J. Peng, Z. Xiong, Y. Zhang, D. Liu, and F. Wu, "Lf-fusion: Dense and accurate 3D reconstruction from light field images," in *IEEE Vis. Comm. Image Process.*, 2017, pp. 1–4.
- [17] H. Zhu, Y. Liu, J. Fan, Q. Dai, and X. Cao, "Video-based outdoor human reconstruction," *IEEE Trans. Circuit Syst. Video Technol.*, pp. 760–770, 2016.
- [18] T. Alldieck, M. Magnor, W. Xu, C. Theobalt, and G. Pons-Moll, "Video based reconstruction of 3D people models," in *IEEE Conf. Comput. Vis. Pattern Recog.*, 2018, pp. 8387–8397.
- [19] S. Saito, Z. Huang, R. Natsume, S. Morishima, A. Kanazawa, and H. Li, "PIFu: Pixel-aligned implicit function for high-resolution clothed human digitization," in *Int. Conf. Comput. Vis.*, 2019, pp. 2304–2314.
- [20] Q. Feng, Y. Liu, Y.-K. Lai, J. Yang, and K. Li, "FOF: Learning fourier occupancy field for monocular real-time human reconstruction," *arXiv preprint arXiv:2206.02194*, 2022.
- [21] H. Zhao, J. Zhang, Y.-K. Lai, Z. Zheng, Y. Xie, Y. Liu, and K. Li, "High-fidelity human avatars from a single RGB camera," in *IEEE Conf. Comput. Vis. Pattern Recog.*, 2022, pp. 15904–15913.
- [22] B. L. Bhatnagar, G. Tiwari, C. Theobalt, and G. Pons-Moll, "Multi-garment net: Learning to dress 3D people from images," in *Int. Conf. Comput. Vis.*, 2019, pp. 5420–5430.
- [23] B. Jiang, J. Zhang, Y. Hong, J. Luo, L. Liu, and H. Bao, "BCNet: Learning body and cloth shape from a single image," in *Eur. Conf. Comput. Vis.*, 2020, pp. 18–35.
- [24] H. Zhu, Y. Cao, H. Jin, W. Chen, D. Du, Z. Wang, S. Cui, and X. Han, "Deep Fashion3D: A dataset and benchmark for 3D garment reconstruction from single images," in *Eur. Conf. Comput. Vis.*, 2020, pp. 512–530.
- [25] E. Corona, A. Pumarola, G. Alenya, G. Pons-Moll, and F. Moreno-Noguer, "Smplicit: Topology-aware generative model for clothed people," in *IEEE Conf. Comput. Vis. Pattern Recog.*, 2021, pp. 11875–11885.
- [26] H. Zhu, L. Qiu, Y. Qiu, and X. Han, "Registering explicit to implicit: Towards high-fidelity garment mesh reconstruction from single images," in *IEEE Conf. Comput. Vis. Pattern Recog.*, 2022, pp. 3845–3854.
- [27] M. Loper, N. Mahmood, J. Romero, G. Pons-Moll, and M. J. Black, "SMPL: A skinned multi-person linear model," *ACM Trans. Graph.*, pp. 1–16, 2015.
- [28] T. Alldieck, M. Magnor, W. Xu, C. Theobalt, and G. Pons-Moll, "Detailed human avatars from monocular video," in *Int. Conf. on 3D Vis.*, 2018, pp. 98–109.
- [29] T. Alldieck, M. Magnor, B. L. Bhatnagar, C. Theobalt, and G. Pons-Moll, "Learning to reconstruct people in clothing from a single RGB camera," in *IEEE Conf. Comput. Vis. Pattern Recog.*, 2019, pp. 1175–1186.
- [30] T. Alldieck, G. Pons-Moll, C. Theobalt, and M. Magnor, "Tex2shape: Detailed full human body geometry from a single image," in *Int. Conf. Comput. Vis.*, 2019, pp. 2293–2303.
- [31] V. Lazova, E. Insafutdinov, and G. Pons-Moll, "360-degree textures of people in clothing from a single image," in *Int. Conf. on 3D Vis.*, 2019, pp. 643–653.
- [32] J. Hu, H. Zhang, Y. Wang, M. Ren, and Z. Sun, "Personalized graph generation for monocular 3D human pose and shape estimation," *IEEE Trans. Circuit Syst. Video Technol.*, pp. 1–1, 2023.
- [33] L. Wang, X. Liu, X. Ma, J. Wu, J. Cheng, and M. Zhou, "A progressive quadric graph convolutional network for 3D human mesh recovery," *IEEE Trans. Circuit Syst. Video Technol.*, pp. 104–117, 2023.
- [34] H. Zhu, X. Zuo, S. Wang, X. Cao, and R. Yang, "Detailed human shape estimation from a single image by hierarchical mesh deformation," in *IEEE Conf. Comput. Vis. Pattern Recog.*, 2019, pp. 4491–4500.
- [35] Z. Zheng, T. Yu, Y. Wei, Q. Dai, and Y. Liu, "DeepHuman: 3D human reconstruction from a single image," in *Int. Conf. Comput. Vis.*, 2019, pp. 7739–7749.
- [36] J. J. Park, P. Florence, J. Straub, R. Newcombe, and S. Lovegrove, "Deepsdf: Learning continuous signed distance functions for shape representation," in *IEEE Conf. Comput. Vis. Pattern Recog.*, 2019, pp. 165–174.

- [37] S. Saito, T. Simon, J. Saragih, and H. Joo, "PIFuHD: Multi-level pixel-aligned implicit function for high-resolution 3D human digitization," in *IEEE Conf. Comput. Vis. Pattern Recog.*, 2020, pp. 84–93.
- [38] Z. Huang, Y. Xu, C. Lassner, H. Li, and T. Tung, "ARCH: Animatable reconstruction of clothed humans," in *IEEE Conf. Comput. Vis. Pattern Recog.*, 2020, pp. 3093–3102.
- [39] T. He, J. Collomosse, H. Jin, and S. Soatto, "Geo-PIFu: Geometry and pixel aligned implicit functions for single-view human reconstruction," *Adv. Neural Inform. Process. Syst.*, pp. 9276–9287, 2020.
- [40] T. He, Y. Xu, S. Saito, S. Soatto, and T. Tung, "ARCH++: Animation-ready clothed human reconstruction revisited," in *Int. Conf. Comput. Vis.*, 2021, pp. 11046–11056.
- [41] Z. Zheng, T. Yu, Y. Liu, and Q. Dai, "PaMIR: Parametric model-conditioned implicit representation for image-based human reconstruction," *IEEE Trans. Pattern Anal. Mach. Intell.*, pp. 3170–3184, 2021.
- [42] Y. Hong, J. Zhang, B. Jiang, Y. Guo, L. Liu, and H. Bao, "StereoPifu: Depth aware clothed human digitization via stereo vision," in *IEEE Conf. Comput. Vis. Pattern Recog.*, 2021, pp. 535–545.
- [43] Y. Cao, G. Chen, K. Han, W. Yang, and K.-Y. K. Wong, "Jiff: Jointly-aligned implicit face function for high quality single view clothed human reconstruction," in *IEEE Conf. Comput. Vis. Pattern Recog.*, 2022, pp. 2729–2739.
- [44] P. Wang, L. Liu, Y. Liu, C. Theobalt, T. Komura, and W. Wang, "Neus: Learning neural implicit surfaces by volume rendering for multi-view reconstruction," *Adv. Neural Inform. Process. Syst.*, vol. 34, pp. 27171–27183, 2021.
- [45] B. Mildenhall, P. P. Srinivasan, M. Tancik, J. T. Barron, R. Ramamoorthi, and R. Ng, "Nerf: Representing scenes as neural radiance fields for view synthesis," in *Eur. Conf. Comput. Vis.*, 2020, pp. 405–421.
- [46] B. Jiang, Y. Hong, H. Bao, and J. Zhang, "Selfrecon: Self reconstruction your digital avatar from monocular video," in *IEEE Conf. Comput. Vis. Pattern Recog.*, 2022, pp. 5605–5615.
- [47] C.-Y. Weng, B. Curless, P. P. Srinivasan, J. T. Barron, and I. Kemelmacher-Shlizerman, "Humannerf: Free-viewpoint rendering of moving people from monocular video," in *IEEE Conf. Comput. Vis. Pattern Recog.*, 2022, pp. 16210–16220.
- [48] S.-Y. Su, F. Yu, M. Zollhöfer, and H. Rhodin, "A-nerf: Articulated neural radiance fields for learning human shape, appearance, and pose," *Adv. Neural Inform. Process. Syst.*, pp. 12278–12291, 2021.
- [49] W. Jiang, K. M. Yi, G. Samei, O. Tuzel, and A. Ranjan, "Neuman: Neural human radiance field from a single video," in *Eur. Conf. Comput. Vis.*, 2022, pp. 402–418.
- [50] Z. Li, Z. Zheng, H. Zhang, C. Ji, and Y. Liu, "Avatarcap: Animatable avatar conditioned monocular human volumetric capture," in *Eur. Conf. Comput. Vis.*, 2022, pp. 322–341.
- [51] J. Chen, Y. Zhang, D. Kang, X. Zhe, L. Bao, X. Jia, and H. Lu, "Animatable neural radiance fields from monocular rgb videos," *arXiv preprint arXiv:2106.13629*, 2021.
- [52] G. Moon, H. Nam, T. Shiratori, and K. M. Lee, "3D clothed human reconstruction in the wild," *arXiv preprint arXiv:2207.10053*, 2022.
- [53] F. Zhao, W. Wang, S. Liao, and L. Shao, "Learning anchored unsigned distance functions with gradient direction alignment for single-view garment reconstruction," in *Int. Conf. Comput. Vis.*, 2021, pp. 12674–12683.
- [54] G. Pons-Moll, S. Pujades, S. Hu, and M. J. Black, "Clothcap: Seamless 4D clothing capture and retargeting," *ACM Trans. Graph.*, pp. 1–15, 2017.
- [55] D. Xiang, T. Bagautdinov, T. Stuyck, F. Prada, J. Romero, W. Xu, S. Saito, J. Guo, B. Smith, T. Shiratori *et al.*, "Dressing avatars: Deep photorealistic appearance for physically simulated clothing," *ACM Trans. Graph.*, pp. 1–15, 2022.
- [56] G. Tiwari, B. L. Bhatnagar, T. Tung, and G. Pons-Moll, "Sizer: A dataset and model for parsing 3D clothing and learning size sensitive 3D clothing," in *Eur. Conf. Comput. Vis.*, 2020, pp. 1–18.
- [57] L. Mescheder, M. Oechsle, M. Niemeyer, S. Nowozin, and A. Geiger, "Occupancy networks: Learning 3D reconstruction in function space," in *IEEE Conf. Comput. Vis. Pattern Recog.*, 2019, pp. 4460–4470.
- [58] O. Halimi, F. Prada, T. Stuyck, D. Xiang, T. Bagautdinov, H. Wen, R. Kimmel, T. Shiratori, C. Wu, and Y. Sheikh, "Garment avatars: Realistic cloth driving using pattern registration," *arXiv preprint arXiv:2206.03373*, 2022.
- [59] M. Habermann, W. Xu, M. Zollhofer, G. Pons-Moll, and C. Theobalt, "Deepcap: Monocular human performance capture using weak supervision," in *IEEE Conf. Comput. Vis. Pattern Recog.*, 2020, pp. 5052–5063.
- [60] Y. Feng, J. Yang, M. Pollefeys, M. J. Black, and T. Bolkart, "Capturing and animation of body and clothing from monocular video," *arXiv preprint arXiv:2210.01868*, 2022.
- [61] L. Qiu, G. Chen, J. Zhou, M. Xu, J. Wang, and X. Han, "REC-MV: Reconstructing 3D dynamic cloth from monocular videos," in *IEEE Conf. Comput. Vis. Pattern Recog.*, 2023, pp. 4637–4646.
- [62] G. Pavlakos, V. Choutas, N. Ghorbani, T. Bolkart, A. A. Osman, D. Tzionas, and M. J. Black, "Expressive body capture: 3D hands, face, and body from a single image," in *IEEE Conf. Comput. Vis. Pattern Recog.*, 2019, pp. 10975–10985.
- [63] Z. Yao, K. Li, Y. Fu, H. Hu, and B. Shi, "GPS-Net: Graph-based photometric stereo network," *Adv. Neural Inform. Process. Syst.*, pp. 10306–10316, 2020.
- [64] Y. Ju, B. Shi, M. Jian, L. Qi, J. Dong, and K.-M. Lam, "Normattention-psn: A high-frequency region enhanced photometric stereo network with normalized attention," *Int. J. Comput. Vis.*, pp. 3014–3034, 2022.
- [65] G. Chen, K. Han, B. Shi, Y. Matsushita, and K.-Y. K. Wong, "Deep photometric stereo for non-lambertian surfaces," *IEEE Trans. Pattern Anal. Mach. Intell.*, pp. 129–142, 2020.
- [66] Y. Liu, Y. Ju, M. Jian, F. Gao, Y. Rao, Y. Hu, and J. Dong, "A deep-shallow and global-local multi-feature fusion network for photometric stereo," *Image Vis. Comput.*, p. 104368, 2022.
- [67] H. Zhang, Y. Tian, X. Zhou, W. Ouyang, Y. Liu, L. Wang, and Z. Sun, "PyMAF: 3D human pose and shape regression with pyramidal mesh alignment feedback loop," in *Int. Conf. Comput. Vis.*, 2021, pp. 11446–11456.
- [68] K. Gong, X. Liang, Y. Li, Y. Chen, M. Yang, and L. Lin, "Instance-level human parsing via part grouping network," in *Eur. Conf. Comput. Vis.*, 2018, pp. 770–785.
- [69] J. Zhang, L. Gu, Y.-K. Lai, X. Wang, and K. Li, "Towards grouping in large scenes with occlusion-aware spatio-temporal transformers," *IEEE Transactions on Circuits and Systems for Video Technology*, pp. 1–1, 2023.
- [70] P. Henderson and V. Ferrari, "Learning single-image 3D reconstruction by generative modelling of shape, pose and shading," *Int. J. Comput. Vis.*, pp. 835–854, 2020.
- [71] H. Bertiche, M. Madadi, and S. Escalera, "PBNS: Physically based neural simulator for unsupervised garment pose space deformation," *arXiv preprint arXiv:2012.11310*, 2020.
- [72] I. Santesteban, M. A. Otaduy, and D. Casas, "SNUG: Self-supervised neural dynamic garments," in *IEEE Conf. Comput. Vis. Pattern Recog.*, 2022, pp. 8140–8150.
- [73] D. P. Kingma and J. Ba, "Adam: A method for stochastic optimization," *arXiv preprint arXiv:1412.6980*, 2014.
- [74] Q. Ma, J. Yang, A. Ranjan, S. Pujades, G. Pons-Moll, S. Tang, and M. J. Black, "Learning to dress 3D people in generative clothing," in *IEEE Conf. Comput. Vis. Pattern Recog.*, 2020, pp. 6469–6478.
- [75] K.-A. Aliev, A. Sevastopolsky, M. Kolos, D. Ulyanov, and V. Lempitsky, "Neural point-based graphics," in *Eur. Conf. Comput. Vis.* Springer, 2020, pp. 696–712.
- [76] S. Prokudin, M. J. Black, and J. Romero, "SmpIpx: Neural avatars from 3D human models," in *IEEE Winter Conf. Appl. Comput. Vis.*, 2021, pp. 1810–1819.
- [77] W. Liu, Z. Piao, J. Min, W. Luo, L. Ma, and S. Gao, "Liquid Warping Gan: A unified framework for human motion imitation, appearance transfer and novel view synthesis," in *Int. Conf. Comput. Vis.*, 2019, pp. 5904–5913.